The Kinetic Mechanism of Ran−Nucleotide Exchange Catalyzed by RCC1

Christian Klebe, Heino Prinz, Alfred Wittinghofer,* and Roger S. Goody

Abteilung Physikalische Biochemie und Strukturelle Biologie, Max-Planck-Institut für molekulare Physiologie, Rheinlanddamm 201, 44139 Dortmund, Germany

Received May 8, 1995; Revised Manuscript Received July 31, 1995[⊗]

ABSTRACT: The interaction of Ran, a Ras-related nuclear GTP-binding protein, with its guanine nucleotide exchange factor RCC1 has been studied by equilibrium and transient kinetic measurements using fluorescent nucleotides. The four-step mechanism of catalyzed nucleotide exchange involves the formation of ternary complexes consisting of Ran, RCC1, and GXP as well as a nucleotide-free dimeric Ran•RCC1 complex. This model is sufficient to describe all experimental data obtained, so that no additional reaction steps must be assumed. All the rate and equilibrium constants for the four-step mechanism have been determined either experimentally or from a simultaneous theoretical fit to all experimental data sets. The affinities of RCC1 to Ran•GDP and Ran•GTP are similar (1.3×10^5 and 1.8×10^5 M^{-1}, respectively) and are high enough to allow formation of the ternary complex under appropriate concentration conditions. In the absence of excess nucleotide and at low Ran concentrations, GDP (or GTP) can be efficiently displaced by excess RCC1 and the ternary complex can be produced. The affinities of both nucleotides (GDP or GTP) to Ran in the corresponding ternary complexes are reduced by orders of magnitude in comparison with the respective binary complexes. The reduction of affinity of both nucleotides in the ternary complexes leads to a dramatic increase in the dissociation rate constants by similar orders of magnitude (from 1.5×10^{-5} s^{-1} to 21 s^{-1} for GDP) and thus to facilitated nucleotide exchange. The quantitative results of the kinetic analysis suggest that the exchange reaction does not per se favor the formation of the Ran•GTP complex, but rather accelerates the formation of the equlibrium dictated by the relative affinities of Ran for GDP/GTP and the respective concentrations of the nucleotide in the cell. The extent of Ran•GTP formation in vivo can be calculated using the constants derived.

GTP-binding proteins are regarded as intracellular molecular switches which operate by cycling between a GDP-bound inactive and a GTP-bound active conformation (Bourne et al., 1990, 1991). The normally slow rate of GTP hydrolysis by such proteins is accelerated by GTPase activating proteins (GAP's),[1] whereas nucleotide exchange is stimulated by guanine nucleotide exchange factors (GEF's) (Boguski & McCormick, 1993). The human GTP-binding protein Ran is involved in nuclear protein transport and probably RNA export (Melchior et al., 1993; Moore & Blobel, 1993; Schlenstedt et al., 1995) and plays a role in cell cycle regulation (Ren et al., 1994; Kornbluth et al., 1994; Clarke et al., 1995). In contrast to many other small GTP-binding proteins, Ran is not isoprenylated at the C-terminus and is mainly located in the nucleus (Bischoff & Ponstingl, 1991a). Its three-dimensional structure has recently been found to be closely related to that of Ras (Scheffzek et al., 1995). The human gene product RCC1 (45 kDa) was originally isolated from a hamster cell line (Ohtsubo et al., 1987) and was shown to function as a GEF for Ran (Bischoff & Ponstingl, 1991b). A human RanGAP1 (65 kDa) has also recently been isolated from HeLa cells (Bischoff et al., 1994), and its basic catalytic properties have been described (Klebe et al., 1995). It was recently found to constitute the mammalian homologue of the RNA1 gene product from yeast *Saccharomyces pombe* and *Saccharomyces cerevisiae* (Becker et al., 1995; Bischoff et al., 1995a). Cytosolic proteins (RanBP, Ran-binding protein) have recently been characterized which bind to Ras in a GTP-dependent manner and are therefore possible effectors of Ran (Lounsbury et al., 1994; Coutavas et al., 1993; Bischoff et al., 1995b).

A mechanism for GEF-catalyzed nucleotide exchange was proposed for $p21^{ras}$ (Powers et al., 1989; Mistou et al., 1991) in analogy to the interaction heterotrimeric G proteins (Bourne et al., 1991) and of elongation factor Tu (EF-Tu) with EF-Ts (Chau et al., 1981; Hwang & Miller, 1985; Romero et al., 1985). It has been shown qualitatively for $p21^{ras}$ that, with catalytic concentrations of GEF, the CDC25 or SDC25 stimulated exchange from GDP to GTP is catalyzed slightly more efficiently than in the reverse direction (Lai et al., 1993; Crechet et al. 1990; Poulet et al., 1994). Likewise, the isolated nucleotide-free complex of Ras•CDC25 can be dissociated more easily by GTP than with GDP (Mosteller et al., 1994).

Relatively little progress has been made toward measuring the individual steps of catalyzed nucleotide exchange of small GNB proteins. Therefore, we are interested in kinetics of the RCC1-catalyzed exchange of Ran-bound nucleotide in terms of a general mechanism, which is likely to apply to most Ras-like GNB proteins. Ran itself, as well as the interacting proteins, provides a good model for mechanistic investigations, partly because the proteins are not posttranslationally modified and interact with each other in the

* Corresponding author.

[⊗] Abstract published in *Advance ACS Abstracts,* September 15, 1995.

[1] Abbreviations: Ran (Ras-like nuclear), protein product of the human Ran/TC4 gene; nfRan, nucleotide-free Ran; RCC1, the product of the human RCC1 (regulator of chromosome condensation) gene; GEF, guanine exchange factor for GTP-binding proteins; GAP, GTPase-activating protein; mGXP, 2′,3′-*O*-bis(*N*-methylanthraniloyl)guanosine di- or triphosphate, the mixture of isomers; mdGXP, 2′-deoxy-3′-*O*-(*N*-methylanthraniloyl)guanosine di- or triphosphate.

0006-2960/95/0434-12543$09.00/0

Scheme 1

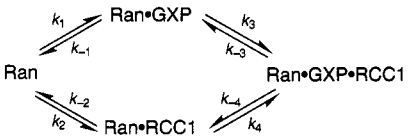

homogeneous solution and not on a membrane surface. In addition to this, the molecular weights of the interacting components are small and can be expressed as full-length proteins in *Escherichia coli*.

The mechanism for interaction of Ran with guanosine nucleotide and RCC1 can be described in the simpliest way in analogy to the interaction of elongation factor-Tu with EF-Ts (Chau et al., 1981) as shown in Scheme 1.

Ran can bind to nucleotide (K_1) or RCC1 (K_2), and both complexes can be isolated in a stable form (Bischoff & Ponstingl, 1991a; Klebe et al., 1993). The interaction of Ran•GXP with RCC1 can be described with two consecutive equilibria describing the formation of ternary complex and nucleotide release, respectively. We have previously reported steady state kinetic studies of the interaction of Ran with either RCC1 or RanGAP1 (Klebe et al., 1995). Here we present methods for equilibrium measurements and transient kinetics which lead to a quantitative discription for the interaction of Ran, RCC1, and nucleotides.

MATERIALS AND METHODS

Proteins and Nucleotides. Expression and isolation of recombinant Ran and RCC1 was as described earlier (Klebe et al., 1993). The concentrated protein solutions (>2 mg/mL) were shock-frozen in liquid nitrogen and stored at −80 °C over 6 months in Tris buffer (64 mM Tris•HCl, pH 7.6, 5 mM dithioerythritol, 5 mM $MgCl_2$) without appreciable loss of activity. Since Ran is usually isolated as a complex with GDP, exchange with other nucleotides was performed as described in Klebe et al. (1995). Nucleotide-free Ran (nfRan) was prepared as described for $p21^{ras}$ (John et al., 1990) with slight modifications. The first step (nucleotide exchange to Ran•GppNHp) was performed in the presence of 200 mM ammonium sulfate and catalytic amounts of RCC1. Ran has been observed to be unstable in the nucleotide-free state but could be stabilized by adding 40% sucrose into the buffer. For reasons which are not yet clear, nucleotide free Ran(Q69L) seems to be more stable than wtRan under identical conditions. Reactions with nfRan(Q69L) were carried out at 10 °C whereas all other measurements were usually done at 25 °C. The nucleotide-free complex of Ran•RCC1 was prepared by mixing a small excess of Ran•GDP with RCC1 in the presence of 10 mM EDTA followed by gel filtration on AcA54 (0.5 × 30 cm) to remove GDP and excess Ran. The buffer used for experiments presented in this study is 30 mM KP_i, pH 7.4, and 5 mM $MgCl_2$ with either 1 mM DTE or 1 mM β-mercaptoethanol. Solutions were degassed and filtered before starting fluorescence assays.

For fluorescence studies, *N*-methylanthraniloyl (mant) derivatives of GDP, GTP, and the corresponding deoxynucleotides were prepared basically as described by Hiratsuka (1983). The products of synthesis were purified by ion exchange chromatography on Q-Sepharose (1.8 × 15 cm) with a gradient of 0.2−0.6 M triethylammonium bicarbonate. Concentrations were determined spectroscopically for nucleotides and by using the standard method described by Bradford (1976) for proteins.

Equilibrium Measurements. Investigations on the interaction between Ran•GXP and RCC1 are not straightforward, since formation of a ternary complex is followed by nucleotide dissociation. A quantitative approach for determining the affinity of Ran•GXP and RCC1 was developed based on a method used for describing the interaction of actin, AppNHp, and subfragment-1 of myosin (Hofmann & Goody, 1978; Greene & Eisenberg, 1978). A 1:1 complex of Ran and mGXP was formed by mixing Ran•GDP with excess mGXP (20-fold) in the presence of 5 mM EDTA, followed by removal of free nucleotide by gel filtration (AcA54, 0.5 × 30 cm) in standard phosphate buffer. The fluorescent complex (1 μM) was titrated with RCC1, by following the decrease of mant fluorescence (excitation 370 nm/emission 450 nm) due to the lower fluorescence yield of non-protein-bound mGXP. After the end point of the titration was reached (i.e., when no further change in fluorescence was observed), unlabeled GXP (50 μM) was added in order to completely displace mGXP still bound to protein and obtain the full amplitude for change in fluorescence (ΔF_{max}). For every titration point, an apparent dissociation constant (K_{app}) was defined between protein-bound and free mGXP. Based on the equilibrum constants for K_1, K_2, and K_4 (defined as association constants) given in Scheme 1, the following equation can be derived (see also eq 1 in Results).

$$K_{app} = \frac{[\text{Ran•RCC1}][\text{mGXP}]}{[\text{Ran•RCC1•mGXP}] + [\text{Ran•mGXP}]} = \frac{1}{K_4 + K_1/(K_2[\text{RCC1}]_{free})} \quad (1)$$

To calculate K_{app}, for every titration point the change in fluorescence relative to the maximal amplitude was used to obtain information about the free concentrations of the different species in solution. Under the assumption that the fluorescence yield is the same for Ran•mGXP and Ran•RCC1•mGXP, the following expression allows the calculation of the amount of protein-bound mGXP:

$$[\text{Ran•RCC1•mGXP}] + [\text{Ran•mGXP}] = [\text{Ran•mGXP}]_0(\Delta F_{max} - \Delta F)/\Delta F_{max}$$

and for free mGXP:

$$[\text{GXP}] = [\text{Ran•RCC1}] = [\text{Ran•GXP}]_0(\Delta F/\Delta F_{max})$$

From the GXP displacement of mGXP bound in the ternary complex at saturating RCC, a value of K_4 can be calculated, since there will be no free Ran•mGXP and the concentration of bound and free mGXP as well as the concentrations of the ternary complex and Ran•RCC1 are known. Thus:

$$K_4 = [\text{Ran•RCC1•mGXP}]/([\text{mGXP}][\text{Ran•RCC1}])$$

Since a 1:1 complex of Ran•mGXP was used,

$$[\text{mGXP}] = [\text{Ran•RCC1}]$$

so that

$$K_4 = [\text{Ran•RCC1•mGXP}]/[\text{mGXP}]^2$$

To use eq 1, the free RCC1 concentration must be calculated in the following manner. The total concentration of RCC1 is given by:

$$[RCC1]_{total} = [RCC1]_{free} + [Ran{\cdot}RCC1] + [Ran{\cdot}RCC1{\cdot}mGXP]$$

The concentration of the ternary complex can be calculated for each point in the titration using the expression given above for K_4, and thus $[RCC1]_{free}$ can be calculated. The apparent dissociation constants for mGXP were calculated according to eq 1 and were plotted against the $[RCC1]_{free}$. Nonlinear fitting to eq 1 then led to values of K_1/K_2 and K_4. The value obtained for K_4 agreed with that obtained directly from the end point of the titration, which shows that the results and evaluation are consistent, but does not in itself give new or better information on the magnitude of K_4. Since the equilibria for possible interactions shown in Scheme 1 are coupled, K_1/K_2 is equal to K_4/K_3, so that a value for K_3 can also be calculated.

Kinetic Measurements. For high time resolution, a stopped-flow apparatus (Hi Tech Scientific, Salisbury, England) was used. The fluorescence of methylanthraniloyl derivatives was excited at 366 nm, and detection was through a cutoff filter at 455 nm. Intrinsic tryptophan fluorescence was followed by excitation at 295 nm (280 nm) and emission through a filter with a cutoff at 320 nm or alternatively with a cutoff at 455 nm for monitoring fluorescence energy transfer between tryptophan and mant residues.

Association of Ran·mdGXP (concentration 0.5 μM) and RCC1 in the absence or presence of excess free nucleotide was followed by monitoring the signal in mant fluorescence or alternatively the fluorescence energy transfer from tryptophan to the mant residue. For each time course, 512 data points were measured. The data were analyzed by fitting the average of 8−10 individual time courses for every RCC1 concentration to a single exponential function, starting after the brief increase in fluorescence seen at the start of the reaction. The observed rate constants (k_{obs}) were plotted against the RCC1 concentration and were secondarily fitted to eq 2 (see Results), from which K_3 and k_{-4} can be calculated.

Association of Ran·RCC1 (0.5 μM) and GXP (>2×b5M) was followed using either mant or tryptophan fluorescence, since for high concentrations of free mdGXP no signal for the reaction can be obtained from monitoring mant fluorescence due to a large background signal. While the change in tryptophan fluorescence was observed to be single exponential, in the case of mant fluorescence the curves proceeds double exponentially. The data obtained for k_{obs} were evaluated as described above.

Association rates of nfRan(Q69L) (0.5 μM) with GXP (>2×b5M) were measured under pseudo first order conditions, although for the lowest concentration (4-fold excess) this is not strictly correct. However, simulations show that the error arising in calculating the pseudo first order rate constant at this excess is only ca. 10%. The reactions were also followed by tryptophan fluorescence. The obtained change in the fluorescence signal during the binding of nucleotide is only about 5% of the total signal. An average of 8 individual experiments results in a sufficient signal to noise ratio for evaluation of the single exponential kinetics.

Numerical Integration. Global analyses of the kinetics of the interaction of the components involved in forming the ternary complexes were carried out using the differential equations corresponding to Scheme 1 (available on request as facsimile files) and the program FACSIMILE (AEA Technology, England). Simultaneous fits were performed as described earlier (Prinz & Maelicke, 1992) with three different data sets. These were the association of five different concentrations of RCC1 to Ran·mdGXP in the absence or presence of excess free GXP, and association of four or five different concentrations of mdGXP to Ran·RCC1. Since the program cannot deal with more than 50 data points for each individual experiment, the number of data points taken for each trigger (512) had to be reduced. In order to ensure that the reaction is accurately represented by the reduced number of data points, the first 10 points were taken directly from the experiment. For the second and third 10 data points, averages of 3 and 10 experimental points were used, respectively. The last 17 data points were averaged from 20 experimental points each. The fluorescence signals for all experiments were calibrated with a standard solution of free mdGXP. All experiments were fitted with the same rate constants and quantum yields. The initial estimates were derived from the interpretation of independent experiments (Figures 1−3). The different concentrations of RCC1 in experiments 1 and 2 (Figure 5) were derived from five consecutive dilutions by (presumably) a factor 2 in the stopped-flow fluorometer. The global fit showed that the dead volume of the reservoir syringes had led to slightly larger dilution factors of 2.34 and 2.37 for experiments 1 and 2, respectively. The amount of fluorescent nucleotide bound to Ran was always measured by HPLC analysis of the protein solution. It was found to agree with the value calculated from the theoretical fit. The concentrations of mdGDP in experiment 3 were derived from the calibration of the fluorescence signal with a standard solution.

RESULTS

The small GNB protein Ran is tightly bound to guanine nucleotides and can be isolated from *E. coli* as a stable 1:1 complex with GDP (Klebe et al., 1993). It has been shown in analogy to $p21^{ras}$ that the release of GDP or GTP is very slow (10^{-4}−10^{-5} s^{-1}; Klebe et al., 1995), and the rate of nucleotide dissociation can be stimulated with a Ran-specific GEF, RCC1 (Bischoff & Ponstingl, 1991b) by a factor of 2 × 10^5 (Klebe et al., 1995). To study the mechanism of nucleotide exchange, we used fluorescent 2′-deoxyguanosine nucleotide analogues labeled with a methylanthraniloyl residue at the 3′-OH group of the ribose (mdGXP). We have shown before that the label does not perturb either the interaction with Ran or the interaction of the Ran−nucleotide complex with RCC1 (Klebe et al., 1995). The structure of Ran shows that the ribose hydroxyl groups are exposed to the solvent (Scheffzek et al., 1995) as found for Ras earlier (Pai et al., 1990).

Equilibrium Measurements of Ran·mGDP with RCC1. The affinity constant of the ternary complex should be such that it can be formed with a reasonable probability at the concentrations of the components in vivo. To obtain a rough estimate of the affinity of the interaction between Ran·GXP with RCC1, we titrated a 1:1 Ran·mGDP complex with increasing amounts of RCC1. By monitoring the decrease in mant fluorescence, we could show directly that the

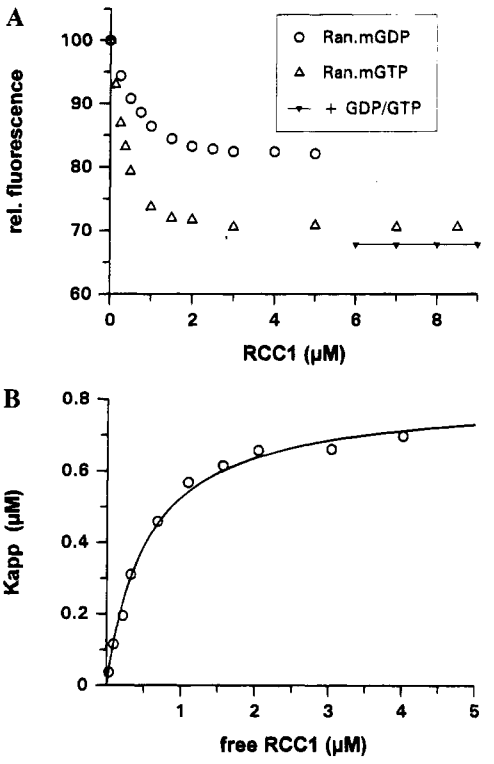

FIGURE 1: (A) Titration of Ran·mGXP complexes with increasing amounts of RCC1. Ran·mGXP complexes were prepared by exchange in the presence of excess nucleotide and subsequent removal of free nucleotide by gel filtration. Increasing amounts of RCC1 were added to 1 μM Ran·mdGXP in 30 mM potassium phosphate buffer (pH 7.4), 5 mM $MgCl_2$, and 1 mM DTE at 25 °C. The decrease of mant fluorescence (excitation 370 nm/emission 450 nm) was followed until the signal remained stable. Nonlabeled nucleotide (50 μM) was added to determine the theoretical end point for total displacement of mdGXP (level indicated by ▼—▼). (B) Plot of the apparent equilibrium constants of fluorescent nucleotide, K_{app}, calculated as described in Materials and Methods, against free RCC1 concentrations for Ran·mGDP (data in panel A). Fitting the data to eq 1 gives information on K_4 and K_1/K_2, defined in Scheme 1 and summarized in Table 1.

nucleotide can be displaced by RCC1 (Figure 1A). When the end point of the titration was reached, addition of excess nonlabeled GDP caused a further decrease of the mant fluorescence. This can be interpreted to mean that displacement of mGXP consists of two successive equilibria, the first being dependent on the RCC1 concentration and the second not. Referring to Scheme 1, at high RCC1 concentrations, Ran is completely saturated with RCC1, but under the conditions used, only partial dissociation of mGDP occurs. Under comparable conditions, a larger amount of Ran-bound mGTP is displaced by RCC1 at the end point of titration.

If we now assume that the yield of mant fluorescence in the Ran·mGDP complex is comparable to that in the ternary complex, a quantitative analysis of the titration data is possible. For each titration point, an apparent equilibrium constant (K_{app}) was defined between the free and protein-bound state of mGDP as described in Materials and Methods. Combining the equilibria shown in Scheme 1, eq 1 can be derived:

$$K_{app} = \frac{[\text{Ran·RCC1}][\text{mGXP}]}{[\text{Ran·RCC1·mGXP}] + [\text{Ran·mGXP}]} = \frac{1}{K_4 + K_1/(K_2[\text{RCC1}]_{free})}$$

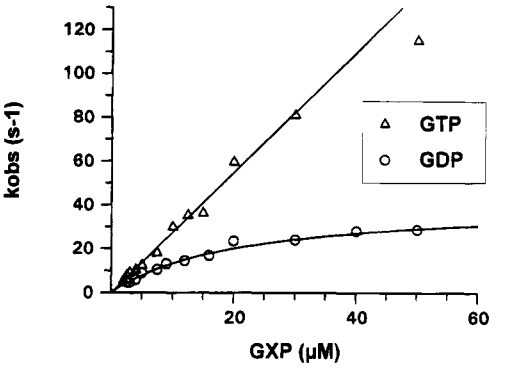

FIGURE 2: Kinetics of association of GXP with nucleotide-free Ran-(Q69L) (0.5 μM). The binding of excess nucleotide under pseudo first order conditions was followed by tryptophan fluorescence (280 nm/cutoff filter 320 nm) at 10 °C in 30 mM KP_i buffer (pH 7.4), 5 mM $MgCl_2$, 1 mM β-mercaptoethanol, and 40% sucrose. The observed single exponential rate constants obtained with different nucleotide concentrations were plotted against nucleotide concentration. The hyperbolic fit for GDP yields a binding constant of 4.7 $\times$ 10^4 M^{-1} for the first step and a maximal velocity of 42 s^{-1} for the second step. The apparent second order rate constants for association at low GXP concentrations are comparable for GDP or GTP ($k_{1(GDP)}$ = 1.9 $\times$ 10^6 M^{-1} s^{-1} and $k_{1(GTP)}$ = 2.6 $\times$ 10^6 M^{-1} s^{-1}).

Table 1: Association Constants Obtained from Equilibrium Measurements of Ran·mdGXP with Increasing Amounts of RCC1

	K_1/K_2	K_3 (10^5 M^{-1})	K_4 (10^5 M^{-1})
Ran·mGDP	0.67	19	12.4
Ran·mGTP	0.07	5.7	0.4

The calculated values of K_{app} were plotted against the concentration of free RCC1 and fitted to eq 1 (Figure 1B). The data obtained for K_4 and the ratio K_1/K_2 (=K_4/K_3) are summarized for mGDP and mGTP in Table 1. Since the affinity between Ran and RCC1 (K_2) is independent of the nature of the nucleotide, the difference in K_1/K_2 for the mGDP and mGTP experiments must reflect a 10-fold higher affinity of Ran for mGDP (K_1) than for mGTP. We have found earlier that the disociation rate constants are 11-fold faster for mGTP than for mGDP (Klebe et al., 1995). This and the values for K_1 support our earlier observation that the nucleotide affinities of Ras-related proteins are mainly dictated by the dissociation rate constants (Goody et al., 1991). The indirectly determined values for K_3 in the cases of mGDP and mGTP seem to be very similar, whereas the value of K_4 is higher for mGDP.

Association of Nucleotide-Free Ran and GXP. We have reported previously that Ran is unstable in the nucleotide-free state and precipitates when diluted to a concentration range which is appropriate for kinetic measurements (Klebe et al., 1995). We have now succeeded in preparing a stable nucleotide-free mutant Ran(Q69L) in a standard phosphate buffer containing 40% sucrose. The stabilizing effect of sucrose has been described for the preparation of stable monomeric nucleotide-free actin by Kasai et al. (1965). The association kinetics of nfRan with guanine nucleotides showed single exponential behavior under pseudo first order conditions. Increasing concentrations of GDP show a hyperbolic dependency of k_{obs} (Figure 2) in a manner which is comparable to that seen for $p21^{ras}$ and is interpreted as reflecting two successive reaction steps (John et al., 1990). It was not possible to reach saturation for the reaction with GTP, but the low value of the apparent second order rate

Table 2: Association and Dissociation Rates of Ran(Q69L) and Nucleotides[a]

	K'_1 (10^4 M^{-1})	k'_2 (s^{-1})	k_1(10^6 M^{-1} s^{-1}) (10 °C)	k_{-1}(10^{-5} s^{-1}) (25 °C)	K_1 (10^{10} M^{-1})
GDP	4.7	41.6	1.9	2.3	16.5
GTP			2.8	21	2.6

[a] The binding constants were calculated assuming a doubling the association rate on shifting from 10 to 25 °C, neglecting the effect of glucose (see text).

constant of GTP binding compared with that expected for a diffusion controlled second order reaction together with the analogy with association kinetics of other GTP-binding proteins suggests that a two-step binding mechanism applies here as well. According to this interpretation, the dissociation constant of the first reaction step appears to be at least 30 μM and the second step at least 120 s^{-1}. The apparent second order rate constants at low concentrations of GDP or GTP at 10 °C were found to be very similar ($k_{1(GDP)}$ = 1.9 × 10^6 M^{-1} s^{-1}; $k_{1(GTP)}$ = 2.8 × 10^6 M^{-1} s^{-1}) since the apparently lower affinity between Ran and GTP in the first step is compensated by a higher value for the second step (>120 s^{-1} compared to 41 s^{-1}; see also Table 2). Use of the concept of an apparent second order rate constant for association at low nucleotide concentrations (i.e., the product of the equilibrium constant for the first step and the forward rate constant for the second step) allows comparison of ligands (or proteins) showing either linear or hyperbolic kinetic behavior, since it is effectively the slope (initial slope in the case of hyperbolic kinetics) of the plot of k_{obs} against concentration.

Since it was not possible to determine association rates at 25 °C, for the purpose of calculating the affinity of Ran and nucleotides, we assumed that the rate obtained at 10 °C would be accelerated by a factor of ca. 2 while shifting to 25 °C. In addition to this, there is likely to be an effect of the high sucrose concentration used on the association kinetics. To obtain an idea of how large this effect might be, we examined the association of mGTP with nucleotide-free Ras p21 in the presence and absence of 40% sucrose. This showed that the increased viscosity led to a reduction of a factor of 3 in the apparent second order rate constant for the association reaction. Thus, the rate constant measured at 10 °C in the presence of 40% sucrose was multiplied by an overall factor of 6 to obtain an estimate of the affinity of Ran for GTP and GDP at 25 °C in the absence of sucrose. Using the rates for GXP dissociation of Ran(Q69L) at 25 °C (Klebe et al., 1995), the affinities between Ran(Q69L) and GXP are calculated as $K_{1(GDP)}$ = 4.9 × 10^{11} M^{-1} and $K_{1(GTP)}$ = 8 × 10^{10} M^{-1}. Hence, the affinity to mGDP is 6-fold higher than to mGTP. Considering the possible difference between wild-type and mutant Ran, this is in reasonable agreement with the results obtained from titration with RCC1, which showed a 10-fold difference in affinities (see Table 1).

Transient Kinetics of the Interaction of Ran·mdGXP and RCC1. For more detailed information concerning the mechanism of RCC1-catalyzed nucleotide exchange, we undertook single turnover experiments using a stopped-flow apparatus. A constant concentration of Ran·mdGXP was mixed with varying excess concentrations of RCC1 and the change in fluorescence recorded. To simplify the analysis, the experiments were performed in the absence of free GDP,

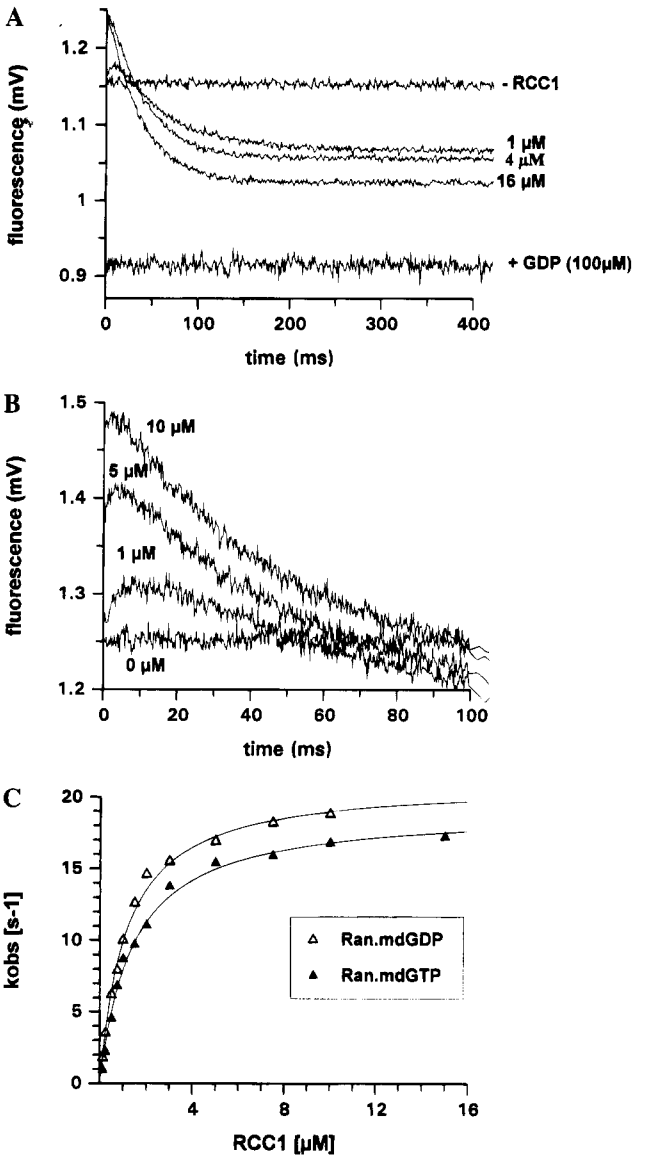

FIGURE 3: (A) Transient kinetics of Ran·mdGDP with RCC1. Time courses of fluorescence obtained after rapidly mixing Ran·mdGDP (0.5 μM) with different concentrations of RCC1 in the absence of free nucleotide were followed by change in mant fluorescence in the buffer 30 mM KP_i (pH 7.4) and 5 mM $MgCl_2$, at 25 °C (excitation 366 nm, cutoff filter GG455). Comparative traces without RCC1 and the end point of the reaction in the presence of 100 μM GDP are indicated. (B) Initial phases of the reactions shown in panel A of this figure. (C) Plot of fitted single exponential rate constants for the second phase of the association reaction against RCC1 concentration. Transient kinetics were performed under conditions described in panel A in the presence of 125 μM free GDP. The data were fitted to eq 2 to give K_3 and k_4 in Scheme 1 (summarized in Table 3).

since under these conditions only two reactions decribed by the equilibrium constants K_3 and K_4 (Scheme 1) are observed.

The observed time curves revealed two phases of the change in fluorescence, a fast increasing and a slower decreasing signal, as shown in Figure 3A. The reaction amplitudes are comparable to the individual points in the equilibrium titration data (Figure 1A) where only part of the Ran-bound nucleotide was displaced by RCC1. The first phase becomes faster in a RCC1 concentration-dependent manner and is no longer detectable for high concentrations, indicating that the association of RCC1 becomes much faster than the dissociation of the ternary complex (Figure 3B). With increasing RCC1 concentrations, the second phase

Table 3: Kinetic Constants for the Interaction of Ran, GXP, and RCC1 Determined by Transient Kinetics Either with Ran•mdGXP and Excess of RCC1 or Alternatively with Ran•RCC1 and Excess of mdGXP

	mdGDP	mdGTP	GDP	GTP
K_3 (10^5 M^{-1})	9.0	7.2		
k_3 (10^7 M^{-1} s^{-1})	5.0	(3.7)		
k_{-3} (s^{-1})	55		73	53
K_4 (10^5 M^{-1})	3.0		3.0	0.5
k_4 (10^6 M^{-1} s^{-1})	6.3	(0.95)		
k_{-4} (s^{-1})	21	19		

becomes saturated and therefore rate limiting, with an observed rate constant of 21 s^{-1} under saturating conditions. The two observed phases for RCC1-catalyzed nucleotide exchange correspond to the model set up from the equilibrium measurements, since the first reaction described by k_3, formation of the ternary complex, would be second order and hence dependent on the RCC1 concentration, whereas the second step is the nucleotide dissoctiation from the ternary complex (k_{-4}) and hence independent of RCC1. The results indicate that the fluorescence yield of the ternary complex must be higher than for the binary Ran•GDP complex.

The same reaction was also carried out in the presence of excess unlabeled nucleotide. Despite the free nucleotide, only the first two reaction steps are observed while monitoring mant fluorescence. Under these conditions (i.e., in the presence of excess unlabeled nucleotide) the second step (nucleotide dissociation) can be considered as irreversible and the displacement of mGDP goes to completion. The second phase is biphasic when Ran-bound mGXP, which is a mixture of 2′- or 3′-mGXP isomers, is used. However, for Ran-bound 2′-deoxy-3′-mGXP (mdGXP), the slow phase is found to follow a single exponential and corresponds to the faster reaction observed with the isomeric mixture, suggesting that the observed biphasic behavior is due to the two isomers of mGXP. We conclude that the fluorescent label must be located on the 3′-position of GDP in order not to interfere with binding. For an initial analysis, we assume that the first step is in relatively rapid equilibrium (not strictly true, but the assumption holds at higher RCC1 concentrations). The observed rate constants for the slow reaction phase should describe a hyperbolic curve with increasing RCC1 concentrations according to the following equation:

$$k_{obs} = \frac{k_{-4}K_3[\text{RCC1}]}{K_3[\text{RCC1}] + 1} \quad (2)$$

The RCC1 concentration dependency of k_{obs} indeed follows a hyperbola (Figure 3C). The values for K_3 and k_{-4} were obtained by fitting the data to eq 2 and are summarized for both Ran•mdGDP and Ran•mdGTP complexes in Table 3. Obviously, in both cases the constants obtained are very similar. For K_3 this was expected from the equilibrium measurements described earlier. On the other hand, the comparable value for k_{-4} suggests that the difference found for K_4 (Table 1) between Ran•GDP and Ran•GTP is mainly due to different association rates of mdGXP to the Ran•RCC1 complex (k_4).

This interpretation would also explain our previous results obtained using catalytic amounts of RCC1 in the exchange reaction. Here it was found that the Michaelis−Menten

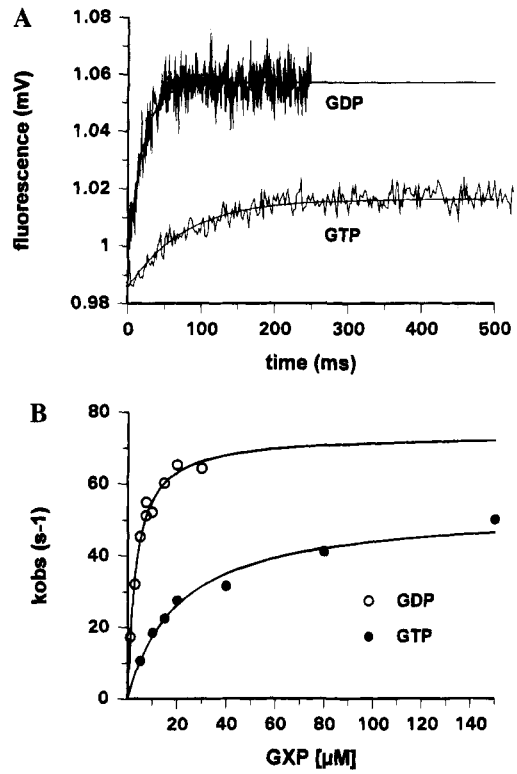

FIGURE 4: (A) Comparison of the association of Ran•RCC1 (0.5 μM; prepared as described under Materials and Methods) with GDP or GTP (5 μM) in potassium phosphate buffer (pH 7.4), 5 mM $MgCl_2$ and 1 mM DTE at 25 °C. The reactions were followed by the change in tryptophan fluorescence (excitation 292 nm, cutoff filter WG320). The traces are fitted to a single exponentiel function. (B) Plots of the observed pseudo first order rate constants obtained from single exponential fits of the association reactions of Ran•RCC1 with different GXP concentrations against GXP concentration of the corresponding reaction. Fitting to eq 2 yielded an estimate of K_4 and an upper limit for k_{-3} (Table 3).

parameters were comparable for exchange of Ran•GDP and Ran•GTP (Klebe et al., 1995). In the case of a large excess of displacing nucleotide with catalytic amounts of RCC1, the product of k_4 and [GXP] becomes large and not rate limiting, and the exchange kinetics are determined solely by K_3 and k_{-4}, which are similar for mdGDP and mdGTP.

Transient Kinetics of the Interaction of Ran•RCC1 and mdGXP. To answer the question whether the kinetics of association of GDP or GTP to the Ran•RCC1 complex are different, we performed the transient kinetic experiment in the reverse direction under pseudo first order conditions. The association of mGDP to Ran•RCC1 revealed a biphasic increasing fluorescence signal. The first reaction step gets very fast (>200 s^{-1}) and is hardly detectable at high nucleotide concentrations (data not shown). The second step becomes saturated with a maximum velocity (k_{-3}) of 55 s^{-1}. Using mdGDP, monophasic behavior was seen, but it was not possible to reach saturating conditions for the reaction rate in the case of mdGTP due to the high background signal at higher nucleotide concentrations. We therefore decided to perform the experiment with nonlabeled nucleotides using the change of intrinsic tryptophan fluorescence as a signal. Under these conditions, we observed single exponential time traces with rate constants corresponding to those of the slow reaction with mdGXP (Figure 4A). We conclude that the fluorescent label must be located on the 3′-position of GXP in order not to interfere with the binding reaction.

Using identical nucleotide concentrations, we find that the association of GTP to Ran•RCC1 is much slower than that of GDP. Quantitative evaluation of the two reaction steps was performed as described before by hyperbolically fitting the secondary plot of k_{obs} against GXP concentration (Figure 4B). However, the first step cannot strictly be considered as a fast pre-equilibrium, and moreover, the second step is reversible, with the back-reaction being second order. Therefore, this kind of experiment gives only a rough estimation of the values of k_{-3} and the association constant K_4 (Table 3). As expected, the maximal rate (k_{-3}) is comparable, whereas the association constant, K_4, was 6-fold higher for GDP due to the faster association reaction (k_4).

Simultaneous Fits of Kinetic Data Sets. The analyses performed so far neccessarily involved assumptions, since the equilibrium and kinetic situations being investigated are complex. We therefore decided to analyze the data rigorously in terms of Scheme 1 using a numerical integration and fitting package (FACSIMILE) which allows fitting of individual rate constants to sets of transient kinetic data. Three sets of previously described kinetic experiments (association of RCC1 to Ran•mGXP in the absence and presence of free excess GXP, and association of GXP to Ran•RCC1) were performed with the same batch of proteins under identical experimental conditions (except for reagent concentrations). Figure 5, panels a−c, shows the results for mdGDP. All time courses were simultaneously fitted to the model of interaction, with initial estimates for the rate constants taken from the analysis described above. When we initially performed the measurements with mGDP, we could not fit a complete set of kinetic experiments. However, when mdGDP was used, the whole set of experiments could be completely described on the basis of Scheme 1 with the rate constants listed in Table 4. The rate constants derived from the simultaneous fits (Table 4) do not differ substantially from the rate constants derived from our initial analysis (Table 3). The relative fluorescence yields of free mdGDP, Ran•mdGDP, and Ran•mdGDP•RCC1 were determined to be 1:1.26:1.42. In the case of mdGTP, the fluorescence of the ternary complex was slightly higher (1.51).

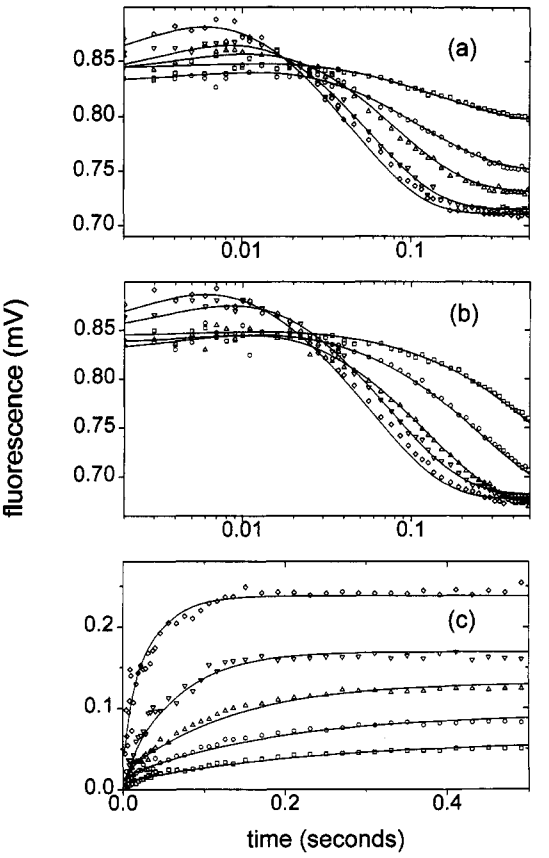

FIGURE 5: Simultaneous computer fitting of 15 kinetic binding experiments performed with Ran, mdGDP, RCC1, and GDP. All experiments were fitted to Scheme 1 with the rate constants listed in Table 4. The fluorescence is shown in mV *vs* time. (a) Association of 450 nM Ran with mdGDP and (□) 133 nM, (○) 310 nM, (△) 728 nM, (▽) 1.707 μM, and (◇) 4 μM RCC1. (b) Exchange reaction: Association of 450 nM Ran occupied to 47% with mdGDP and (□) 127 nM, (○) 302 nM, (△) 714 nM, (▽) 1.69 μM, and (◇) 4 μM RCC1 in the presence of 100 μM GDP. (c) Association of 305 nM of the complex Ran•RCC1 with (□) 117 nM, (○) 222 nM, (△) 450 nM, (▽) 1.339 μM, and (◇) 2.898 μM mdGDP. The fluorescence increase (minus background) observed after the addition of the fluorochrome is shown.

Table 4: Kinetic Constants Determined by Numerical Integration and Simultaneous Evaluation of 14 Different Time Courses Using the Program FACSIMILE

	mdGDP	mdGTP
K_1 (10^{10} M^{-1})	16	0.74
k_1 (10^6 M^{-1} s^{-1})	1.9	1.0
k_{-1} (10^{-5} s^{-1})	1.2	14
K_2 (10^{11} M^{-1})	4.0	4.0
K_3 (10^6 M^{-1})	1.35	1.85
k_3 (10^6 M^{-1} s^{-1})	74.4	102
k_{-3} (s^{-1})	55	55
K_4 (10^5 M^{-1})	5.4	0.34
k_4 (10^6 M^{-1} s^{-1})	11.4	0.65
k_{-4} (s^{-1})	21.1	19

DISCUSSION

The biological activity of GTP-binding proteins in the cell depends on the nature of the nucleotide bound at their active sites. Here we present several different methods based on fluorescence techniques which allow, for the first time, a quantitative description of the GEF-catalyzed nucleotide exchange on a Ras-like GTP-binding protein.

In the initial equilibrium experiments, which were important for designing the stopped-flow kinetic experiments, titration of Ran•mGXP complexes with RCC1 in the absence of excess GXP showed that nucleotide displacement was not complete, even at high (saturating) RCC1 concentrations (Figure 1A). Thus, depending on the starting concentration of Ran•mGXP and on the nature of the mGXP (i.e., whether it is mGDP or mGTP), a fraction of the nucleotide remains bound. This demonstrates the existence of a ternary complex and gives information on the dissociation constant of the respective nucleotide from this ternary complex. Quantitative evaluation of the equilibrium measurements was performed assuming that the fluorescence yields of Ran•mGXP and Ran•RCC1•mGXP are identical. This is not strictly true, as shown by the results of Figure 3B, so the initial analysis can only be regarded as approximate. However, it reveals that the affinity between Ran•mGDP and RCC1 is of the same order as between the Ran•RCC1 complex and mGDP. This allows the nucleotide exchange reaction to proceed in either direction, depending on the relative free concentrations of RCC1 and nucleotide. Surprisingly, the affinity of Ran•RCC1 for mGTP is found to be lower than for mGDP, which favors the reaction of the binary complex Ran•RCC1

with GDP. The results also show that the difference in affinity of GDP and GTP in the the ternary complexes reflects a similar difference in the absence of RCC1; i.e., Ran has an approximately 10-fold higher affinity for GDP than for GTP. The higher affinity of Ran for GDP than for GTP is different from the situation in $p21^{ras}$, where it has been shown that binding of GTP is 3- or 12-fold tighter than that of GDP (John et al., 1990; Neal et al., 1988).

The proposed simple model for RCC1-catalyzed nucleotide exchange is supported by kinetic investigations of the nucleotide displacement with excess RCC1. Two phases were observed in this reaction, in which the initial increase in fluorescence could be correlated with the binding of RCC1. This could indicate that, on binding of RCC1, the environment of the mant residue becomes more hydrophobic and hence the fluorescence yield increases. This interpretation does not neccessarily imply that RCC1 binds near to the nucleotide binding site of Ran. The association binding constants for RCC1 to either Ran·GDP or Ran·GTP are very similar, as are the dissociation rates of the nucleotides from the ternary complex formed. The main difference between GDP and GTP is found in the association rate of nucleotide to the Ran·RCC1 complex, indicating that in vivo the relative concentrations of GDP and GTP determine the amount of activated Ran produced.

Comparing the association constants determined from equilibrium measurements (Table 1) or transient kinetics (Table 3), the values for GTP show better agreement than those for GDP. There are two possible reasons for this discrepancy. (i) The quantitative evaluation of the titration experiments was performed upon the assumption that the fluorescence yield of the mant residue bound either to Ran alone or to the Ran·RCC1 complex is comparable. As shown in Figure 3A, this is not the case. Since the amount of ternary complex produced is much larger in the case of GDP, the corresponding error should be larger than for GTP. (ii) The association reactions of Ran·RCC1 with nucleotide were evaluated by the same approach as that used for the reaction of Ran·GXP with RCC1 in the presence of free GXP. However, this approach is not strictly correct, first because there is not a very fast pre-equilibrium and second because the dissociation step is reversible. Hence, a formally correct interpretation of the observed kinetics with classical methods is not possible. We therefore analyzed the kinetic experiments using a numerical integration and fitting method taking into account the individual differential equations corresponding to Scheme 1. This procedure was done simultaneously with three sets of experiments carried out under standardized conditions, using as starting values the constants obtained from the equilibrium and kinetic experiments. The results (some fitted curves are shown in Figure 5, and the results are summarized in Table 4 and Figure 6) show that Scheme 1 is indeed sufficient for a quantitative description of the kinetic experiments and that no further assumptions concerning additional steps need be made. However, as demonstrated by Figure 2, the association of GDP to nucleotide-free Ran actually involves an additional step which is not included in Scheme 1. Direct evidence for a step of this sort was observed in the association of mdGXP to Ran·RCC1. It is possible that the rate constant attributed to dissociation of RCC1 from the ternary complex is in fact an isomerization of the ternary complex which is equivalent to the second step in the association of nucleotide with Ran and that subsequent dissociation of RCC1 is very fast in comparison. According to this interpretation, the underlying mechanism of acceleration of nucleotide dissociation by RCC1 is due to a reversal of the second step seen in the binding of nucleotide to Ran, with subsequent dramatic reduction in affinity. In this respect, it is of interest to note that the affinity of GDP in the ternary complex is only about 1 order of magnitude higher than the affinity of the first binding step of GDP to Ran alone.

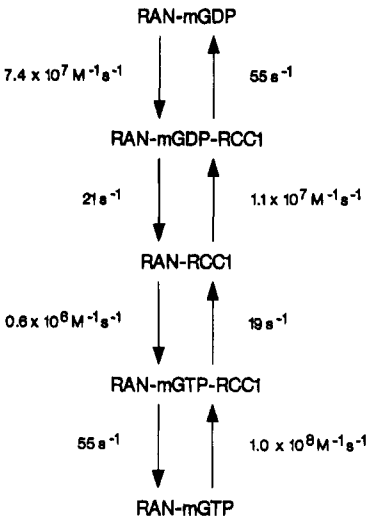

FIGURE 6: Kinetic scheme for the guanine nucleotide exchange reaction, with Ran·mdGDP as the educt and mdGTP as the product of the reaction, using the kinetic data of Table 4.

The rate constants given in Table 4 are used to describe kinetically the exchange reaction of Ran·mGDP to yield Ran·mGTP (Figure 6). This shows again that only the association reaction of GXP with the Ran·RCC1 complex shows any major difference between GDP and GTP, which would favor, unexpectedly, the formation of the Ran·GDP complex. For Ras it has been found, although no intrinsic rate constants have been measured, that the addition of GTP to the Ras−CDC25 complex is favored severalfold over the addition of GDP (Mosteller et al., 1994). This indicates that guanine nucleotide exchange factors act as catalysts that speed up the equlibrium formation between the GDP- and GTP-bound state of the GTP-binding proteins. The cellular content of active GTP-bound protein is dictated only by the respective affinities for GDP/GTP and the concentrations of these nucleotides in the cell. The total intracellular concentrations of GTP and GDP were determined in the case of hepatocytes to be 327 and 91 μM, respectively (Kleinecke et al., 1979). The intracellular Ran concentration has been reported to be 6 μM and in 25-fold excess over RCC1 (Bischoff & Ponstingl, 1991a). Simulations based on these intracellular concentrations, in combination with the determined rate constants for the interaction of Ran with nucleotides and RCC1, revealed that a maximum of 38% GTP-bound Ran can be formed. The fact that the local concentration of Ran in the nucleus might be higher than the total cellular concentation does not alter this conclusion, since the simulations show that the relative amount of formed Ran·GTP is independent of the absolute Ran concentration, as long as this is significantly lower than the nucleotide concentration, which seems likely. This suggests that, in addition to the regulation of Ran by proteins such as GAP and RCC1, the intracellular concentrations of GTP and GDP

could influence the biological activity mediated by Ran•GTP. It is also possible that the presence of Ran-binding proteins, some of which have been identified (Lounsbury et al., 1994; Coutavas et al., 1993; Bischoff et al., 1995b), shifts the equilibrium further toward formation of the Ran−GTP complex.

The maximal rate for RCC1 stimulated nucleotide exchange on Ran at high RCC1 concentrations was found to be ca. 20 s^{-1}, and Figure 6 shows that the release of nucleotide from the ternary complex is the rate-limiting step in either direction. This is not in good quantitative agreement with our steady state measurements of the GDP/mGDP exchange using catalytic amounts of RCC1, which led to a value of 5 s^{-1} (Klebe et al., 1995). We have calculated the Michaelis−Menten constants K_M and k_{cat} for an enzymatic reaction with four consecutive reversible reaction steps (Johnson, 1992). The reaction of RCC1-catalyzed nucleotide exchange of Ran•GDP in the presence of 100 μM free mdGDP was calculated using the rate constants shown in Table 4, assuming that there is no difference between GDP and mdGDP. In the case of K_M (1.1 μM), there was excellent agreement with experimental data (also 1.1 μM). However, k_{cat} was calculated to be 14.9 s^{-1} compared to $k_{cat(exp)} = 5$ s^{-1}. This discrepancy could be due to partially inactivated RCC1, since steady state kinetics are dependent on the total concentration of RCC1. The titration experiment (Figure 1) suggests that the 3-fold difference in k_{cat} cannot be explained simply by inactivated RCC1 because the nucleotide can be completely dissociated by a 2-fold excess of RCC1. However, the difference is so small that, in view of the different nature of the experiments performed in the two experimental approaches, we conclude that there are no compelling reasons for considering a more complex scheme than that shown in Scheme 1, although it is likely that additional steps, which are kinetically "silent" (see below), are involved.

The data reported here do *not* give direct information on the structural mechanism of the mutual reduction of affinities of nucleotide and exchange factor in the ternary complex. However, the very existence of a ternary complex means that the two species do not compete directly for the same site on Ran, which is not surprising in view of their different nature, and the easiest interpretation of this is that the binding sites for GXP and RCC1 are either spatially distinct or partially overlapping. The properties of such a system could then be described by a simple general mechanism of facilitated dissociation (Prinz & Striessnig, 1993). This mechanism takes into account that high affinity reversible binding can be regarded as the product of a number of low affinity interactions between ligands and protein. If RCC1 binds (with low affinity) in the vicinity of the nucleotide binding site, competition between RCC1 and GXP for individual weak interactions becomes feasible. This would then lead to a stepwise conformational change from ran (high nucleotide, low RCC1 affinity) to RAN (low nucleotide, high RCC1 affinity), as indicated in Scheme 2. Since these individual conformational changes could be fast and spectroscopically silent, they might not be identified directly in our experiments. Instead, the whole array of ternary complexes would appear as an ensemble of states. Fast dissociation of GXP is possible from the RCC1-induced conformation (RAN), whereas fast dissociation of RCC1 will

Scheme 2

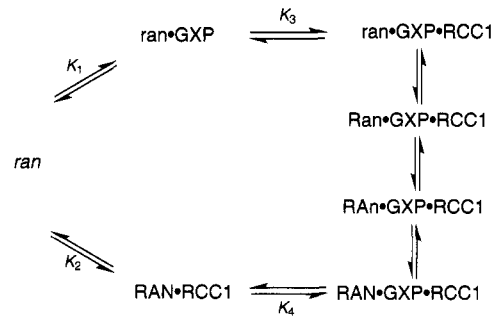

occur from the nucleotide-induced conformation (ran) in Scheme 2.

It should be noted that this scheme is formally identical for spatially distinct or partially overlapping sites. We cannot distinguish between these two cases with presently available information, and it will be necessary to determine the structure of a Ran•RCC1 complex. However, the data on the rate of association of GDP and GTP to the Ran•RCC1 complex suggest that the nucleotide binding site is easily available to its (nucleotide) ligand even in the Ran•RCC1 complex. Thus, the composite second order rate constant is at least as high as to Ran alone (for GDP even higher), which would be most readily explained if the nucleotide binding site is not partially blocked.

Actomyosin is a system which has similar properties with respect to the mutually exclusive binding of nucleotide and actin to myosin. Here structural data show very clearly that the actin binding site on the myosin head is remote from the ATP binding site (Rayment et al., 1993a,b). The analogy between this and the Ran−RCC1 system is striking, since the main effect of actin is to accelerate the rate of release of the products of ATP hydrolysis from myosin by factors of ca. 10^3 (for inorganic phosphate) and ca. 10^2 (for ADP). In contrast to the interaction of Ras-like proteins with their exchange factors, this turns myosin into an efficient ATPase, in the classical sense of the term, since ATP cleavage on myosin is fast and does not require a GAP-like activity. Thus, the combination of myosin and actin can be regarded as analogous to the combination of a Ras-like protein, its GAP, and its exchange factor.

REFERENCES

Becker, J., Melchior, F., Gerke, V., Bischoff, F. R., Ponstingl, H., & Wittinghofer, A. (1995) *J. Biol. Chem.* (in press).

Bischoff, F. R., & Ponstingl, H. (1991a) *Proc. Natl. Acad. Sci. U.S.A. 88*, 10830−10834.

Bischoff, F. R., & Ponstingl, H. (1991b) *Nature 354*, 80−82.

Bischoff, F. R., Klebe, C., Kretschmer, J., Wittinghofer, A., & Ponstingl, H. (1994) *Proc. Natl. Acad. Sci. U.S.A. 91*, 2587−2591.

Bischoff, F. R., Krebber, H., Smirnova, E., Dong, W., & Ponstingl, H. (1995a) *EMBO J. 14*, 705−715.

Bischoff, F. R., Krebber, H., Kempf, T., Hermes, I., & Ponstingl, H. (1995b) *Proc. Natl. Acad. Sci. U.S.A.* (in press).

Boguski, M. S., & McCormick, F. (1993) *Nature 366*, 643−654.

Bourne, H. R., Sanders, D. A., & McCormick, F. (1990) *Nature 348*, 125−132.

Bourne, H. R., Sanders, D. A., & McCormick, F. (1991) *Nature 349*, 117−127.

Bradford, M. M. (1976) *Anal. Biochem. 72*, 284−253.

Chau, V., Romero, G., & Biltonen, R. L. (1981) *J. Biol. Chem. 256*, 5591−5596.

Clarke, P. R., Klebe, C., Wittinghofer, A., & Karsenti, E. (1995) *J. Cell Sci.* (in press).
Coutavas, E., Ren, M., Oppenheim, J. D., D'Eustachio, P., & Rush, M. (1993) *Nature 366*, 585−587.
Crechet, J. B., Poullet, P., Mistou, M. Y., Parmeggiani, A., Camonis, J., Boy-Marcotte, E., Damak, F., & Jaquet, M. (1990) *Science 248*, 866−868.
Eccleston, J. F., Kanagasabai, T. F., & Geeves, M. A. (1988) *J. Biol. Chem. 263*, 4668−4672.
Goody, R. S., Frech, M., & Wittinghofer, A. (1991) *Trends Biochem. Sci. 16*, 327−328.
Greene, L. E., & Eisenberg, E. (1978) *Proc. Natl. Acad. Sci. U.S.A. 75*, 54−58.
Hiratsuka, T. (1983) *Biochim. Biophys. Acta 742*, 496−508.
Hofmann, W., & Goody, R. S. (1978) *FEBS Lett. 89*, 169−172.
Hwang, Y. W., & Miller, D. L. (1985) *J. Biol. Chem. 260*, 11498−11502.
John, J., Sohmen, R., Feuerstein, J., Linke, R., Wittinghofer, A., & Goody, R. S. (1990) *Biochemistry 29*, 6058−6065.
Johnson, K. A. (1992) *Enzymes 20*, 1−61.
Kasai, M., Nakano, E., & Oosawa, F. (1965) *Biochim. Biophys. Acta 94*, 494−503.
Klebe, C., Nishimoto, T., & Wittinghofer, A. (1993) *Biochemistry 32*, 11923−11928.
Klebe, C., Bischoff, R., Ponstingl, H., & Wittinghofer, A. (1995) *Biochemistry 34*, 639−647.
Kleinecke, J., Düls, C., & Söling, H. D. (1979) *FEBS Lett. 107*, 198−202.
Kornbluth, S., Dasso, M., & Newport, J. (1994) *J. Cell Biol. 125*, 705−719.
Lai, C. C., Boguski, M., Broek, D., & Powers, S. (1993) *Mol. Cell. Biol. 13*, 1345−1352.
Lounsbury, K. M., Beddow, A. L., & Macara, I. G. (1994) *J. Biol. Chem. 269*, 11285−11290.
Melchior, F., Paschal, B., Evans, J., & Gerace, L. (1993) *J. Cell Biol. 123*, 1649−1659.
Mistou, M.-Y., Jacquet, E., Poullet, P., Rensland, H., Gideon, P., Schlichting, I., Wittinghofer, A., & Parmeggiani, A. (1992) *EMBO J. 11*, 2391−2398.
Moore, M. S., & Blobel, G. (1993) *Nature 365*, 661−663.
Mosteller, R. D., Han, J., & Broek, D. (1994) *Mol. Cell. Biol. 14*, 1104−1112.
Neal, S. E., Eccleston, J. F., Hall, A., & Webb, M. R. (1988) *J. Biol. Chem. 263*, 19718−19722.
Ohtsubo, M., Kai, R., Furuno, N., Sekiguchi, T., Sekiguchi, M., Hayashida, H., Kuma, K-i., Miyata, T., Fukushige, S., Murotsu, T., Matsubara, K., & Nishimoto, T. (1987) *Genes Dev. 1*, 585−593.
Pai, E. F., Krengel, U., Petsko, G. A., Goody, R. S., Kabsch, W., & Wittinghofer, A. (1990) *EMBO J. 9*, 2351−2359.
Poullet, P., Lin, B., Esson, K., & Tamanoi, F. (1994) *Mol. Cell. Biol. 14*, 815−821.
Powers, S., O'Neill, K., & Wigler, M. (1989) *Mol. Cell. Biol. 9*, 390−395.
Prinz, H., & Maelicke, A. (1992) *Biochemistry 31*, 6728−6738.
Prinz, H., & Striessnig, J. (1993) *J. Biol. Chem. 268*, 18580−18585.
Rayment, I., Rypniewski, W. R., Schmidt-Bäse, K., Smith, R., Tomchick, D. R., Benning, M. M., Winkelmann, D. A., Wesenberg, G., & Holden, H. M. (1993a) *Science 261*, 50−58.
Rayment, I., Holden, H. M., Whittaker, M., Yohn, C. B., Lorenz, M., Holmes, K. C., & Milligan, R. A. (1993b) *Science 261*, 58−65.
Ren, M., Coutavas, E., D'Eustachio, P., & Rush, M. G. (1994) *Mol. Cell. Biol. 14*, 4216−4224.
Romero, G., Chau, V., & Biltonen, R. L. (1985) *J. Biol. Chem. 260*, 6167−6174.
Scheffzek, K., Klebe, C., Fritz-Wolf, K., Kabsch, W., & Wittinghofer, A. (1995) *Nature* (in press).
Schlenstedt, G., Saavedra, C., Loeb, J. D. J., Cole, C. N., & Silver, P. A. (1995) *Proc. Natl. Acad. Sci. U.S.A. 92*, 225−229.

BI951030V